

Original Article

Cite this article: França LM, dos Santos PC, Barroso WA, Gondim RSD, Coêlho CFF, Flister KFT, and Paes AMA. (2020) Post-weaning exposure to high-sucrose diet induces early non-alcoholic fatty liver disease onset and progression in male mice: role of dysfunctional white adipose tissue. *Journal of Developmental Origins of Health and Disease* **11**: 509–520. doi: [10.1017/S2040174420000598](https://doi.org/10.1017/S2040174420000598)

Received: 15 November 2019

Revised: 15 May 2020

Accepted: 28 May 2020



First published online: 29 June 2020

Keywords:

Carbohydrates; white adipose tissue; free fatty acids; lipogenesis; childhood

Address for correspondence: Antonio Marcus de Andrade Paes, Universidade Federal do Maranhão, Departamento de Ciências Fisiológicas, Avenida dos Portugueses, 1966, Campus Dom Delgado, CEP: 65.080-805, São Luís, MA, Brazil. Email: marcuspaes@ufma.br

Post-weaning exposure to high-sucrose diet induces early non-alcoholic fatty liver disease onset and progression in male mice: role of dysfunctional white adipose tissue

Lucas Martins França¹ , Pâmela Costa dos Santos¹, Wermerson Assunção Barroso², Roberta Sabrine Duarte Gondim¹, Caio Fernando Ferreira Coêlho¹, Karla Frida Torres Flister¹ and Antonio Marcus de Andrade Paes¹ 

¹Laboratory of Experimental Physiology (LeFisio), Department of Physiological Sciences, Federal University of Maranhão (UFMA), São Luís, MA, Brazil and ²Laboratory of Medical Investigation (LIM-51), Department of Emergency Medicine, School of Medicine, University of São Paulo (FMUSP), São Paulo, SP, Brazil

Abstract

Non-alcoholic fatty liver disease (NAFLD) is the hepatic manifestation of metabolic syndrome, ranging from simple steatosis to non-alcoholic steatohepatitis (NASH) particularly among chronic consumers of added sugar-rich diets. However, the impact of early consumption of such diets on NAFLD onset and progression is unclear. Thus, this study sought to characterise metabolic factors involved in NAFLD progression in young mice fed with a high-sucrose diet (HSD). Male Swiss mice were fed HSD or regular chow (CTR) from weaning for up to 60 or 90 days. Obesity development, glucose homeostasis and serum biochemical parameters were determined at each time-point. At day 90, mice were euthanised and white adipose tissue (WAT) collected for lipolytic function assessment and liver for histology, gene expression and cytokines quantification. At day 60, HSD mice presented increased body mass, hypertriglyceridemia, peripheral insulin resistance (IR) and simple steatosis. Upon 90 days on diet, WAT from HSD mice displayed impaired insulin sensitivity, which coincided with increased fasting levels of glucose and free fatty acids (FFA), as well as NAFLD progression to NASH. Transcriptional levels of lipogenic genes, particularly stearoyl-CoA desaturase-1, were consistently increased, leading to hepatic leukocyte infiltration and pro-inflammatory cytokines spillover. Therefore, our dataset supports IR triggering in the WAT as a major factor for dysfunctional release of FFA towards portal circulation and consequent upregulation of lipogenic genes and hepatic inflammatory onset, which decisively concurred for NAFLD-to-NASH progression in young HSD-fed mice. Notwithstanding, this study forewarns against the early introduction of dietary sugars in infant diet, particularly following breastfeeding cessation.

Introduction

Metabolic syndrome (MetS) is defined as a set of cardiometabolic disorders including at least three out of the following: central obesity, hypertriglyceridemia, fasting hyperglycaemia, hyperinsulinaemia and hypertension.¹ These comorbidities have been more associated with individual lifestyle than with heredity because inheritance contributes less than 2% for obesity and 5%–10% for type 2 diabetes mellitus.^{2,3} However, increasing evidence has supported that most metabolic disorders are programmed before adulthood, as consequence of environmental and nutritional insults occurring at early stages of life, such as gestation, lactation and childhood.^{4,5} For instance, the worldwide epidemic growth of MetS has been directly associated with the exponential rise in sugar consumption during the last decades.^{6,7} This issue is particularly important for infants and children, given that sugars are a major component of their diet, representing nearly 25% of total energy intake in the childhood.⁸ Although the accountable mechanisms are barely known, they conceptually fall within the developmental origins of health and disease (DOHAD) theory, which is currently recognised as an important contributor to the epidemic MetS.⁵

In the liver, MetS manifests as non-alcoholic fatty liver disease (NAFLD), whose prevalence reaches 25% of general population, but may affect up to 80% of obese subjects.⁹ Ranging from simple steatosis to non-alcoholic steatohepatitis (NASH), NAFLD has also been correlated to the elevated dietary intake of sugars.¹⁰ Sucrose consumption stimulates *de novo* lipogenesis (DNL), triacylglycerol (TAG) synthesis and NAFLD development through mechanisms orchestrated by two main lipogenic transcriptions factors: carbohydrate regulatory element-binding

protein (ChREBP) and sterol regulatory element-binding protein 1c (SREBP1c).¹¹ ChREBP is directly activated by glucose and fructose, whereas SREBP1 responds to higher serum insulin levels evoked by excess sucrose intake.¹² In a previous report, we showed that exposure of weaned mice to an isocaloric high-sucrose diet (HSD) for 90 days increased transcriptional levels of both ChREBP and SREBP1 in a time-dependent manner with consequent NAFLD onset, but no progression into NASH.¹³

The close relationship between obesity and NAFLD has been ascribed to the direct involvement of white adipose tissue (WAT), which releases a variety of bioactive substances, such as free fatty acids (FFA), leptin, adiponectin and inflammatory cytokines. Ultimately, these adipokines exert important paracrine and endocrine functions on energy balance and metabolic homeostasis.¹⁴ Hypertrophic WAT favours the development of local insulin resistance (IR) and consequent increase in circulating FFA, which are uptaken by the liver and esterified to directly render TAG synthesis and consequent fat accumulation into hepatocytes.¹⁵ However, whether sucrose intake impacts WAT homeostasis in a way that reverberates on molecular and functional mechanisms involved in NAFLD-to-NASH progression is scarcely known.

Thus, in the current study we hypothesised that early exposure to an isocaloric 25% sucrose diet since weaning up to young adulthood disrupts WAT homeostasis generating metabolic factors involved in NAFLD-to-NASH progression. Data herein presented strongly support the triggering of IR in the WAT as a major factor for dysfunctional release of FFA towards portal circulation and consequent upregulation of DNL genes and hepatic inflammatory onset, which concurred for NAFLD-to-NASH progression in young HSD-fed mice. Furthermore, our data advocate for the urgent establishment of sucrose consumption limits worldwide, particularly at childhood, to prevent precocious onset of NAFLD in the youth.

Methods

Experimental design and diet composition

Weaned male (12.8 ± 0.3 g) Swiss mice (*Mus musculus*) provided by the animal facility house of the Federal University of Maranhão (UFMA) were randomised into two groups: one fed a high-sucrose but isoenergetic diet (HSD, *n* = 12) for 60 and 90 days, and the other fed a standard chow (CTR, *n* = 12 - Nuvilab®, Curitiba (PR), Brazil) for the same period. At each time-point, half the group was euthanised, resulting in six mice per time per group. HSD was adapted from de Lima *et al.*¹⁶ and manufactured with powdered standard chow (40%), condensed milk (40%), refined sugar (8.5%) and filtered water *qsp* for a final mixture containing 65% total carbohydrates (25% sucrose), 12.3% proteins and 4.3% total lipids, totalling 14.6 kJ/g. The standard chow contained 55.4% total carbohydrates (10% sucrose), 21% proteins and 5.2% total lipids, totalling 14.7 kJ/g.

Animals were kept at animal facility house of Biological and Health Sciences Center (CCBS, UFMA), at three mice per cage (polycarbonate, 30 × 20 × 13 cm), at a temperature of 23 ± 2 °C, 12-h light/dark cycle, and access to filtered water and HSD or standard chow *ad libitum*. Throughout experimental periods, body weight (g) and energy intake (kJ/day/10 g bw) were assessed twice a week, when the whole food (~200 g per cage) was replaced. Feed efficiency was calculated as the quotient of weekly body weight gain/weekly energy intake (g/kJ). All procedures were performed in accordance with the rules of Brazilian Council for the Control of Animal Experimentation and approved by the

Ethical Committee on Animal Use and Welfare of UFMA under ruling number 23115.002832/2017-25.

Evaluation of obesity, blood and tissues collection

During every 30 days of experimental period, obesity development was assessed by Lee Index calculation, which is the quotient of the cube root of body weight (g) per naso-anal length (cm).¹⁷ Upon 60 and 90 days on diet, animals were submitted to 9 h overnight fasting, anaesthetised (10 mg/kg xylazine + 40 mg/kg ketamine, *i.p.*) and submitted to laparotomy for blood collection by cardiac puncture. After coagulation (30 min, 25°C), serum samples were obtained by centrifugation (1300 × *g*, 15 min, 4°C) and stored at -80°C for further analysis. Periepididymal and retroperitoneal WAT and interscapular brown adipose tissue (BAT) pads were removed and weighed for fat accumulation assessment. The liver was also collected, washed out with PBS and separated into four portions: one was immediately immersed in 10% formalin for histological studies and three were frozen (-80°C) for fat liver content assessment, RNA extraction and cytokines measurements.

Assessment of glucose homeostasis and serum biochemical profile

Nine-hour fasted mice (six per group) were orally administered 2 g/kg glucose for performance of oral glucose tolerance test (oGTT).¹⁸ Capillary blood drops were collected by tail cut immediately before (time 0) and 15, 30, 60 and 120 min after glucose load and blood glucose concentrations measured through glucometer (Accucheck Active®, Roche Diagnostic, Mannheim (BW), Germany). Insulin resistance was inferred from the calculation of TyG Index (TyG = Ln [fasting triglycerides (mg/dl) × fasting glucose (mg/dl)]/2).¹⁹ Serum samples were used for measurement of glucose, TAG and FFA, and total cholesterol (TC) levels were measured by colorimetric method (spectrophotometry) using sensitive and specific commercial kits according to manufacturer's instructions (Labtest®, Lagoa Santa (MG), Brazil).

Assessment of ex vivo lipolytic activity of white adipose tissue

Lipolytic activity was evaluated according to Vaughan²⁰ using six animals per group. Periepididymal adipose tissue samples (~100 mg) were sectioned into small fragments and incubated in Krebs buffer (120 mM NaCl; 15 mM NaHCO₃; 4.83 mM KCl; 1.2 mM MgSO₄; 1.21 mM KH₂PO₄; 2.4 mM CaCl₂; 1% BSA and 0.1% glucose after pH adjustment to 7.4) under pumping aeration for 1 h (37°C) in the absence (basal) and presence of 20 μM isoproterenol (Sigma-Aldrich, St. Louis (MO), USA) or 20 μM insulin (Sigma-Aldrich, St. Louis (MO), USA). After incubation, the reactions were stopped in ice bath and supernatant collected for glycerol concentration spectrophotometric measurement using a TAG-specific commercial kit, as described above.

Assessment of hepatic lipid profile

Liver samples (500 mg) were homogenised in 5 ml of chloroform/methanol (2:1) solution and left to stand overnight (4–8°C) for extraction of total fats. Then, the tissue was filtered off and the filtrate added 0.9% NaCl (saline 1:5 filtrate). This mixture was stirred, allowed to stand for 2 h and centrifuged (100 × *g*, 5 min) for separation of the methanol and chloroform phases. 1 ml of chloroform phase was collected and air-dried, leaving only the

Table 1. Primers sequences

| Gene* | Forward primer | Reverse primer | Amplicon (bp) | GenBank |
|-----------------|-----------------------------|------------------------------|---------------|----------------|
| SREBP-1c | 5'-GGCTGTTGTCTACCATAAGC-3' | 5'-ATGTCCTCTGTGTACTTGC-3' | 61 | NM_011480.4 |
| ChREBP | 5'-TTAGTTCCTGAGCAGAGAGG-3' | 5'-ACTAGTGCAAAGGCAAGAG-3' | 58 | NM_021455.4 |
| PPAR-γ | 5'-TTTTCAAGGGTGCCAGTTTC-3' | 5'-CGCAGGTTTTTGAGGAATC-3' | 67 | NM_001127330.2 |
| PPAR-α | 5'-ATGCCAGTACTGCCGTTTTC-3' | 5'-GGCCTTGACCTGTTCATGT-3' | 40 | NM_001113418.1 |
| FASN | 5'-TGGAAAGATAACTGGGTGAC-3' | 5'-AGAACCAGAATGGATACCT-3' | 60 | NM_007988.3 |
| SCD-1 | 5'-AAAAGTGGACATGTCTGACC-3' | 5'-TACCTCCTCTGGAACATCAC-3' | 57 | NM_009127.4 |
| DGAT-2 | 5'-ACGCAGTCACCCTGAAGAACC-3' | 5'-GGAACCCTCCTCAAAGATCACC-3' | 85 | NM_026384.3 |
| β2M | 5'-CATGGCTCGCTCGGTGACC-3' | 5'-AATGTGAGGCGGGTGAACCTG-3' | 92 | NM_009735 |

*Abbreviations: SREBP-1c, sterol response element-binding protein-1c; ChREBP, carbohydrate-responsive element-binding protein; PPAR-γ, peroxisome proliferator-activated receptor-γ; PPAR-α, peroxisome proliferator-activated receptor-α; FASN, fatty acid synthase; SCD-1, stearoyl-CoA desaturase-1; DGAT-2, diacylglycerol acetyltransferase-2; β2M, beta-2-microglobulin.

solid fat mass, which was weighed and expressed as total fat (mg) per tissue mass (g).²¹ The solid fat mass was resuspended in 1 ml Triton-X 100/methanol (2:1) and thoroughly homogenised for the measurement of TAG and TC concentrations, as described above, whose values were extrapolated to be expressed as TAG or TC (mg) per tissue mass (g), reflecting their relative proportions in the total extracted fat.

Analysis of hepatic histology

Liver samples previously fixed in 10% formalin underwent dehydration, diaphanisation and paraffin inclusion, for posterior cut of 5 μm thickness slices using a microtome and staining with hematoxylin and eosin (H&E). The slices were analysed under light microscopy (100× and 400×) by two researchers in an independent blind manner according to the NAFLD activity score (NAS) criteria, which grade three main features [steatosis (0–3), lobular inflammation (0–3) and hepatocellular ballooning (0–2)], to reach a total score ranging from 0 to 8.²² When discrepant scores were attributed to the same sample, a third pathologist gave the casting vote in a blind way. Average values for each feature were used for statistical comparison between HSD mice and its respective age-matched CTR group.

Hepatic gene expression by real-time polymerase chain reaction

RNA samples (3 μg) were extracted from liver samples ($n = 6$) using Trizol reagent (Invitrogen, Germany), as per manufacturer instruction, and converted to cDNA using Super Script II Reverse Transcriptase (Invitrogen, Germany). The quantitative polymerase chain reaction (qPCR) amplification was performed by 7500 Real-Time PCR (Applied Biosystems, USA) using Platinum SYBR Green qPCR SuperMix-UDG (Invitrogen, Germany) for detection. Reactions were incubated at 50°C for 2 min and 95°C for 2 min followed by 40 cycles of 95°C for 15 s and 60°C for 1 min. To melt curve stage, reactions were incubated at 95°C for 15 s, 60°C for 60 min and 95°C for 15 s. Primers for DNL-related transcription factors and enzymes genes amplification (Table 1) were designed using Primer Express software (Applied Biosystem, USA) and manufactured by Invitrogen, Brazil. Samples were normalised to the relative levels of β-2 microglobulin (β2M), and results expressed as the fold change (FC) values of $2^{-\Delta\Delta CT}$.

Quantification of hepatic cytokines

Liver samples (~ 100 mg) were homogenised in RIPA lysis buffer (10 mM Tris HCl pH 7.5; 1% sodium deoxycholate; 1% Triton X-100; 150 mM NaCl; 0.1% SDS) plus protease inhibitors (1 mg/ml pepstatin A; 100 mM PMSF). The homogenates were centrifuged (14,000 × g, 10 min, 4 °C) and 50 μl of each sample was used for the determination of cytokines tumour necrosis factor-α (TNF-α), interleukin-6 (IL-6) and interleukin-10 (IL-10) by enzyme-linked immunosorbent assay (ELISA) according to the manufacturer's instructions (R&D System, Minneapolis (MN), USA). Results were expressed as variation (Δ) of hepatic cytokines levels on HSD mice in relation to age-matched CTR mice.

Statistical analysis

Sample size was calculated using free software G * Power 3.1²³ (Heinrich-Heine University Düsseldorf, Düsseldorf (NRW), Germany) with setting the power of study in 80%, significant level 5% and effect size determined with means and standard deviation from a previous study with HSD.²⁴ Results were expressed as mean ± standard error of the mean (SEM). Shapiro-Wilk test was applied for normality assuring. The comparisons between the two groups, in each time-point, were performed by Student's *t*-test and the differences were significant when $p < 0.05$. All statistical analyses were performed with the software Prism 7.0 (GraphPad, San Diego (CA), USA).

Results

Obesity development

HSD mice presented higher weight gain than CTR, which started to be statistically significant by 15 days on diet and reached differences as high as 16% at 60 days and 20% at 90 days of dietary intervention (Fig. 1a). Interestingly, HSD was 20% more efficient in promoting weight gain (Fig. 1c), although energy intake by HSD mice had been 18% lower than CTR (Fig. 1b). The Lee index, which indicates mice's body mass, was 6% higher in HSD than CTR at 30 days on diet, remaining 6% and 9% higher at 60 and 90 days of nutritional intervention, respectively (Fig. 1d). Accordingly, HSD intake resulted in greater time-dependent fat accumulation in all collected fat pads. Upon 60 days on diet, HSD mice showed retroperitoneal (Fig. 2a) and periepididymal (Fig. 2b) fat pads 26% and 70% higher than CTR, respectively, while a 33% increase was

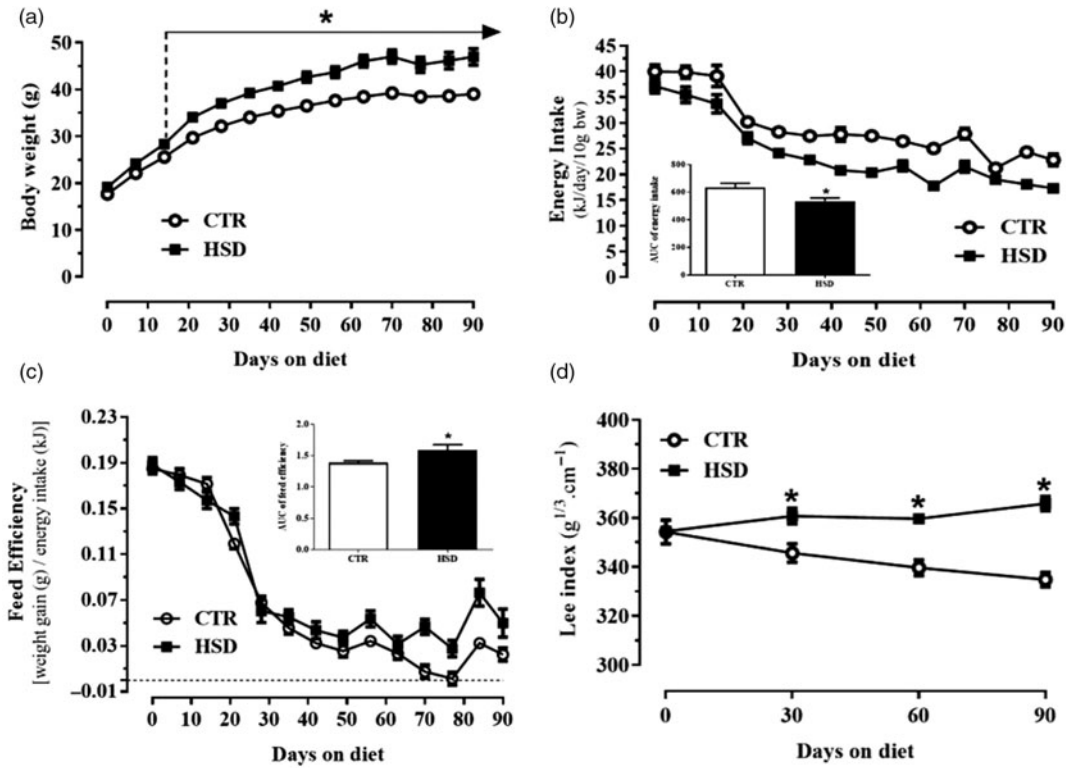


Fig. 1. Weight, food and morphometric monitoring. Body weight (a), energy intake (b), feed efficiency (c) and Lee index (d) were evaluated in mice fed with standard chow (CTR) or high-sucrose but isoenergetic diet (HSD) for 90 days. Dots and bars represent mean \pm SEM and the differences between the groups were analysed by Student's *t*-test. The dotted line indicates where the difference between the groups begins (A). **p* < 0.05. *n* = 06 per time per group.

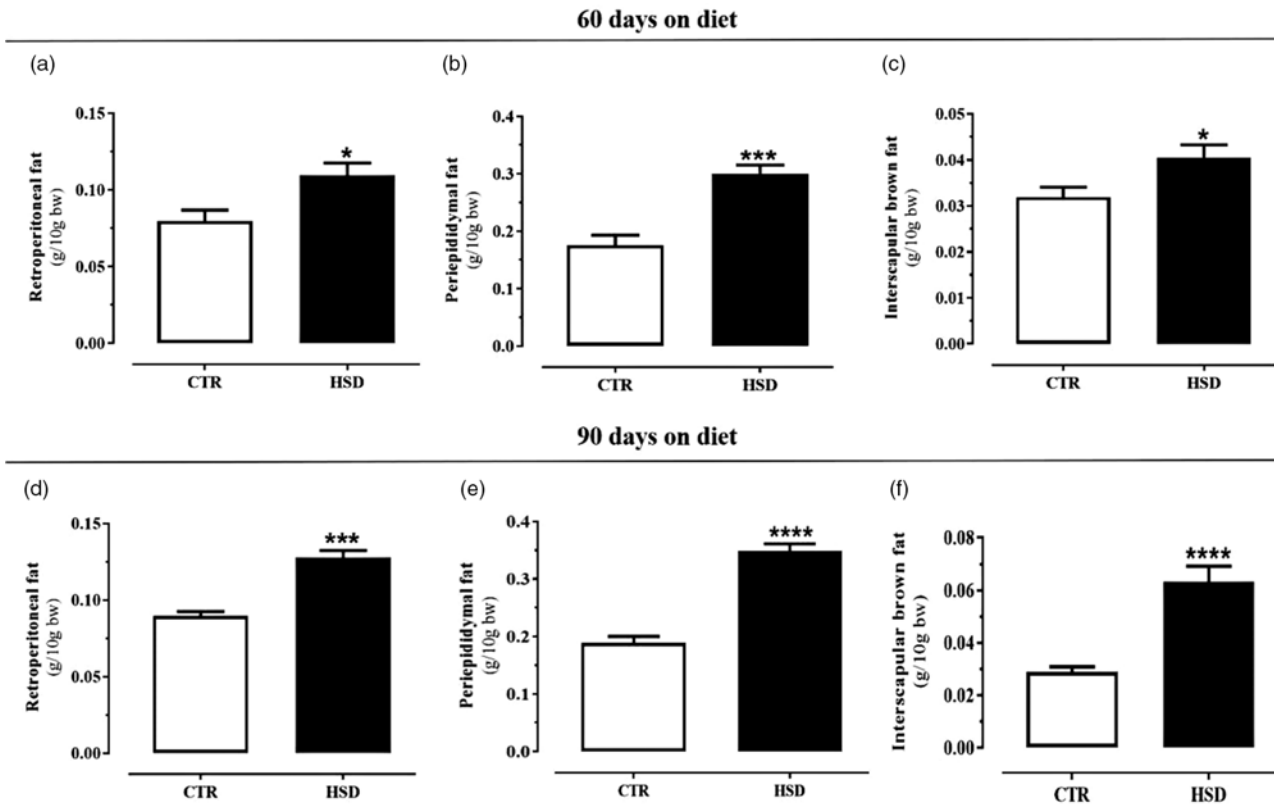


Fig. 2. Adipose tissue fat pads accumulation. Relative weights of retroperitoneal (a and d) and periepididymal (b and e) white adipose tissue, as well as interscapular brown adipose tissue (c and f) pads collected from mice fed with standard chow (CTR) or high-sucrose but isoenergetic diet (HSD) for 60 or 90 days. The bars represent mean \pm SEM and the differences between the groups analysed by Student's *t*-test. **p* < 0.05. ****p* < 0.0001 vs. CTR. *n* = 6 per time per group.

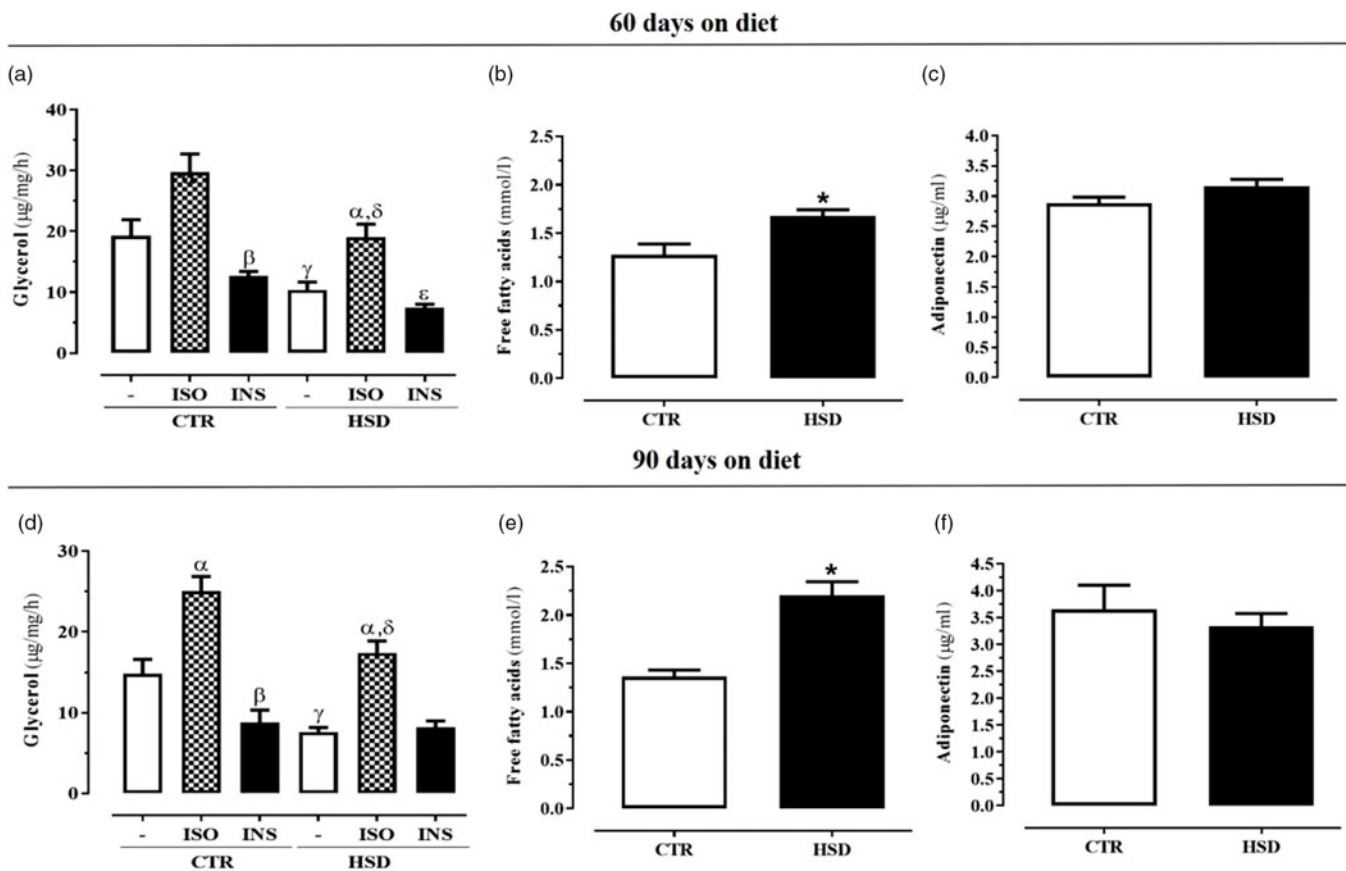


Fig. 3. White adipose tissue function. Lipolytic activity of periepididymal white adipose tissue (a and d) and serum concentrations of free fatty acids (b and e) and adiponectin (c and f) of mice fed with standard chow (CTR) or high-sucrose but isoenergetic diet (HSD) for 60 or 90 days. Lipolytic activity (a and d) was evaluated by glycerol release rates of *ex vivo* adipose tissue isolated at baseline (-) and incubated with 20 μ M isoproterenol (ISO) or 20 μ M insulin (INS). The bars represent mean \pm SEM and the differences between the groups analysed by Student's *t*-test. *HSD vs. CTR; †ISO vs. (-) and INS; ‡CTR + INS vs. CTR -; §HSD - vs. CTR -; ¶HSD + ISO vs. CTR + ISO; ††HSD + INS vs. HSD -. ^{†, ‡, §, ¶, ††} $p < 0.05$. $n = 6$ per time per group.

verified in interscapular BAT (Fig. 2c). Exposure to HSD for 90 days expanded those fat depots, with increases of 46%, 85% and 125% in the retroperitoneal (Fig. 2d), periepididymal (Fig. 2e) and interscapular (Fig. 2f) fat pads, respectively, as compared to CTR group.

White adipose tissue function

To further assess the effects of HSD on adiposity, we evaluated the lipolytic activity of periepididymal fat pad, as well as its secretory function. Assessment of *ex vivo* lipolytic activity showed that HSD consumption significantly impaired lipolytic response in both basal and stimulated conditions at 60 (Fig. 3a) and 90 days (Fig. 3d) on diet, as compared to CTR. This is supported by the lower glycerol release found in WAT from HSD mice when the tissue was stimulated with 20 μ M isoproterenol, with reductions of 36% at 60 and 32% at 90 days on diet in relation to the response found in isoproterenol-stimulated CTR (Fig. 3a, 3d, respectively). Noteworthy, HSD mice had preserved sensitivity to anti-lipolytic effect of insulin at 60 days on diet (Fig. 3a), an effect consistently impaired at 90 days (Fig. 3d).

In parallel, HSD mice had serum FFA levels 30% higher than CTR (Fig. 3b) at 60 days, evolving to values 62% higher at 90 days (Fig. 3e), which implies a twofold increase of serum FFA levels within the short course of 30 days. On the contrary, there was no difference in serum adiponectin levels throughout the dietary

intervention (Fig. 3c, 3f). This set of data supports an early WAT dysfunction characterised by the impairment of insulin action and consequent increase in FFA release into bloodstream; although displaying unaltered serum adiponectin levels, which suggests the absence of cytokines overflow.

Insulin–glucose axis function

At 60 days on diet, HSD mice did not have altered fasting glycaemia (Fig. 4a), although presented glucose intolerance, depicted from the oGTT (Fig. 4b), as well as impaired peripheral insulin sensitivity, demonstrated by increased TyG Index values (Table 2). Upon additional 30-days on diet, HSD mice presented fasting serum glucose levels 20% higher than age-matched CTR mice (Fig. 4c), which coursed with deeper impairment of both glucose intolerance (Fig. 4d) and insulin sensitivity, assessed through TyG Index calculation (Table 2). Interestingly, the rising of fasting glycaemia coincided with the development of IR in the WAT (Fig. 3d), but not with the onset of peripheral IR, as presumed from TyG Index data.

Hepatic and serum lipids profile

Data on Table 2 also show that HSD intake caused intense lipid accumulation in both serum and liver. Hepatic total fat in HSD mice was augmented in both time-points, reaching levels 54% higher than CTR at 90 days on diet. Measurement of hepatic

Table 2. Lipid profiles of liver and serum biochemical parameters, as well as TyG index values of weaned mice fed with standard chow (CTR) or high-sucrose diet (HSD) for 60 and 90 days

| Lipid profiles | 60 days on diet | | 90 days on diet | |
|------------------------------|-----------------|----------------------------|-----------------|----------------------------|
| | CTR | HSD | CTR | HSD |
| Liver (mg/g of liver) | | | | |
| Total fat | 393.0 ± 20.65 | 473.0 ± 26.00 ^a | 252.7 ± 12.35 | 388.9 ± 15.51 ^y |
| Cholesterol | 3.2 ± 0.10 | 4.5 ± 0.38 ^a | 4.0 ± 0.45 | 8.1 ± 0.63 ^y |
| Triacylglycerol | 3.6 ± 0.35 | 6.08 ± 0.27 ^y | 5.8 ± 0.79 | 14.9 ± 1.92 ^y |
| Serum (mmol/l) | | | | |
| Cholesterol | 2.29 ± 0.09 | 3.00 ± 0.17 ^β | 2.98 ± 0.09 | 3.73 ± 0.16 ^y |
| Triacylglycerol | 0.42 ± 0.02 | 0.62 ± 0.06 ^β | 0.46 ± 0.05 | 0.95 ± 0.07 ^y |
| TyG index | 8.02 ± 0.10 | 8.56 ± 0.09 ^β | 7.82 ± 0.08 | 8.51 ± 0.17 ^β |

Data represent mean ± SEM and were analysed by Student's *t*-test. ^a*p* < 0.05; ^β*p* < 0.01 and ^y*p* < 0.0001 vs. CTR. *n* = 6.

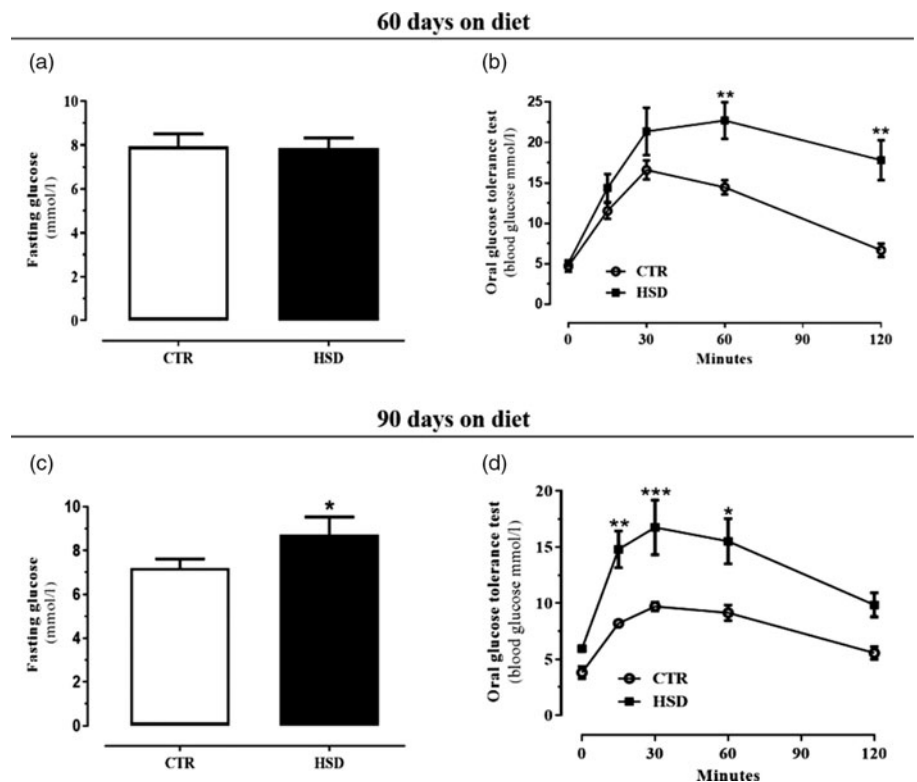


Fig. 4. Glucose homeostasis. Fasting glucose levels (a and c) and oral glucose tolerance test (oGTT) (b and d) of mice fed with standard chow (CTR) and high-sucrose but isoenergetic diet (HSD) for 60 or 90 days. oGTT (8-h fasting) was performed at 0 times (baseline) and 15, 30, 60 and 120 min after glucose *bolus* (2 g/kg). Dots and bars represent mean ± SEM and the differences between the groups analysed by Student's *t*-test. **p* < 0.05; ***p* < 0.01; ****p* < 0.0001 vs. CTR. *n* = 6 per time per group.

TAG and TC showed a significant increase between groups, but the relative amount in HSD versus CTR was expanded in a time-dependent manner (Table 2). In accordance, serum TAG and TC levels were proportionally augmented in HSD mice in both time-points, reaching levels 100% and 25% higher, respectively, in comparison to CTR, at 90 days on diet (Table 2). The greater effect of HSD on hepatic TAG synthesis and secretion strongly supports the establishment of IR in the liver, an outcome that corroborates TyG Index values (Table 2).

NAFLD activity score (NAS)

Microscopic analysis of H&E-stained liver slices according to the NAFLD activity score described by Kleiner *et al.*²² showed that, upon 60 days on diet, HSD mice only presented simple hepatic

steatosis (Fig. 5). However, at 90 days on diet it was verified the presence of hepatocyte ballooning and leukocyte inflammatory infiltration in addition to microvesicular steatosis, which characterise HSD mice as suffering from NASH (Fig. 5).

Gene expression of hepatic lipid metabolism markers

To evaluate the effects of HSD on lipid metabolism in the liver, we performed the gene expression of DNL transcription factors (Fig. 6) and enzymes (Fig. 7). At 60 days on diet, the only upregulated gene was that for peroxisome proliferator-activated receptor- α (*PPAR- α*) expression (Fig. 6c). However, upon 30 days of additional exposure to HSD (day 90), HSD mice showed an average twofold upregulation of all the assessed DNL transcription factors: *ChREBP*, *SREBP-1c* and peroxisome proliferator-activated

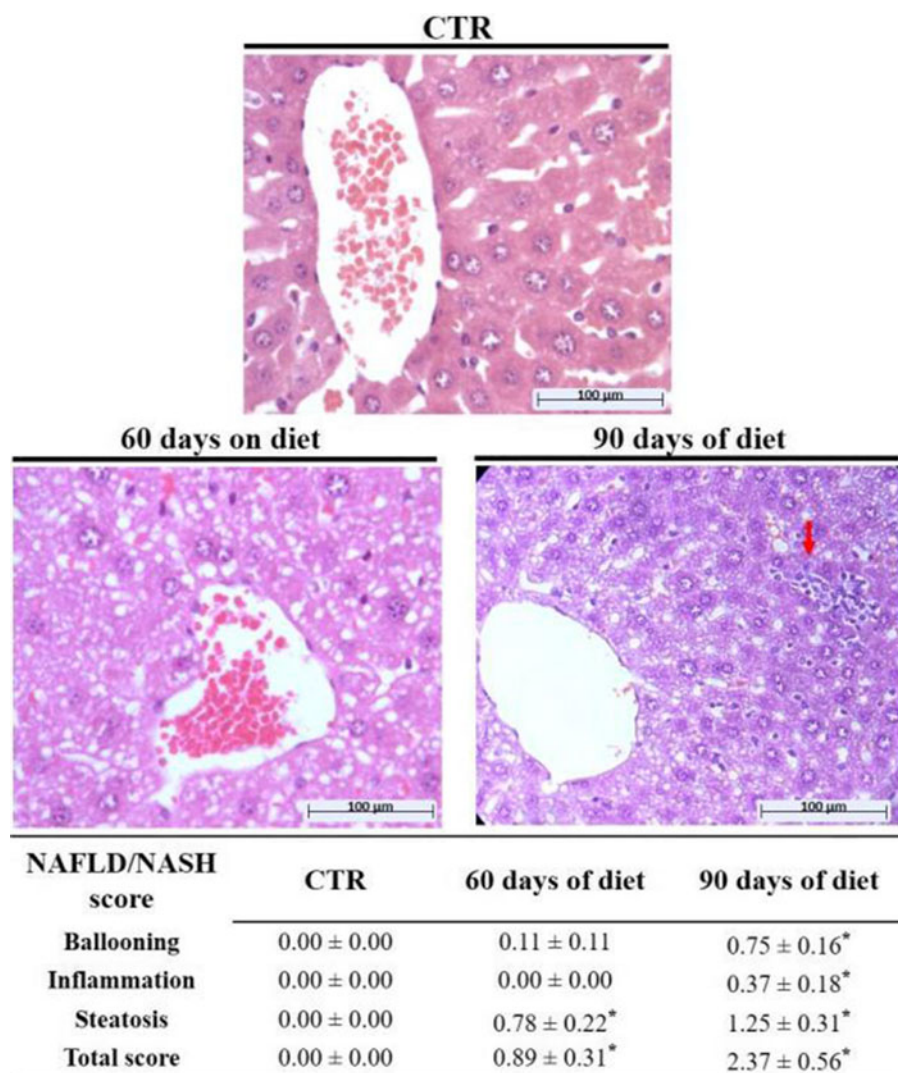


Fig. 5. Liver histology. Liver histology from mice fed with standard chow for 90 days (CTR) or high-sucrose but isoenergetic diet (HSD) for 60 or 90 days. Representative sections (10 μ m) of the liver of these animals stained with H&E are shown in the panel above. Each slide was classified according to the NAFLD/NASH score. The red arrow indicates inflammatory focus. Data are expressed as mean \pm SEM and the difference between groups determined by Student's *t*-test. **p* < 0.05 vs. CTR. *n* = 6 per time per group.

receptor- γ (*PPAR*- γ), in addition to maintaining increased *PPAR*- α gene expression (Fig. 6e–h). In relation to the assessed lipogenic enzymes, the only alteration found in HSD mice was the increased expression of stearoyl-CoA desaturase-1 (*SCD*-1) in both times. Importantly, *SCD*-1 transcriptional levels expanded from a three-fold increase at 60 days (Fig. 7c) to roughly more than fivefold increase at 90 days of HSD exposure (Fig. 7f), while fatty acid synthase (*FASN*) and diacylglycerol acetyltransferase-2 (*DGAT*-2) transcriptional levels did not change.

Hepatic inflammatory cytokines profile

There was no difference in the hepatic concentrations of *TNF*- α , *IL*-6 and *IL*-10 between groups at 60 days on diet, as compared to age-matched CTR group (Fig. 8a–c). However, corroborating NAS data (Fig. 5), 90 days' exposure to HSD increased the expression of *TNF*- α (Fig. 8d), *IL*-6 (Fig. 8e) and *IL*-10 (Fig. 8f) in 39%, 16% and 19%, respectively, in relation (Δ) to age-matched CTR groups.

Discussion

Many studies have used sugar-rich diets to evaluate metabolic programming of offspring through dams' exposure during gestation or lactation.^{5,25} However, the post-weaning period is much less

investigated, even being considered a critical window for developmental programming.²⁶ Moreover, most studies using mono- or disaccharide-rich diets have focused on total energy intake instead of the nutritional composition of such diets.^{25,27,28} Therefore, in this study we applied a high-sucrose but isoenergetic diet (HSD) since weaning through young adulthood to assess mid-term metabolic factors involved in NAFLD-to-NASH progression. Our data show that 60-day exposure to HSD promoted adipose tissue expansion associated with dyslipidaemia and simple hepatic steatosis. However, extending exposure time to 90 days resulted in the development of IR in the WAT, with consequent increase in FFA release, upregulation of lipogenic genes and establishment of hepatic inflammation, which led NAFLD to progress towards NASH.

Post-weaning exposure to excess sucrose promptly promoted weight gain in our HSD mice, leading them to show increased body mass by the two time-points herein determined, 60 and 90 days on diet. Distinctly from Wistar rats, which are much harder to get fatty under the same diet,^{24,29} Swiss mice showed themselves to be very susceptible to this dietary intervention. Interestingly, this speedy weight gain occurred despite the fact they had a lower energy intake throughout the experimental time. This is reliably explained by the action of the sucrose- and lactose-derived glucose, contained in HSD as table sugar and condensed milk, on hypothalamic

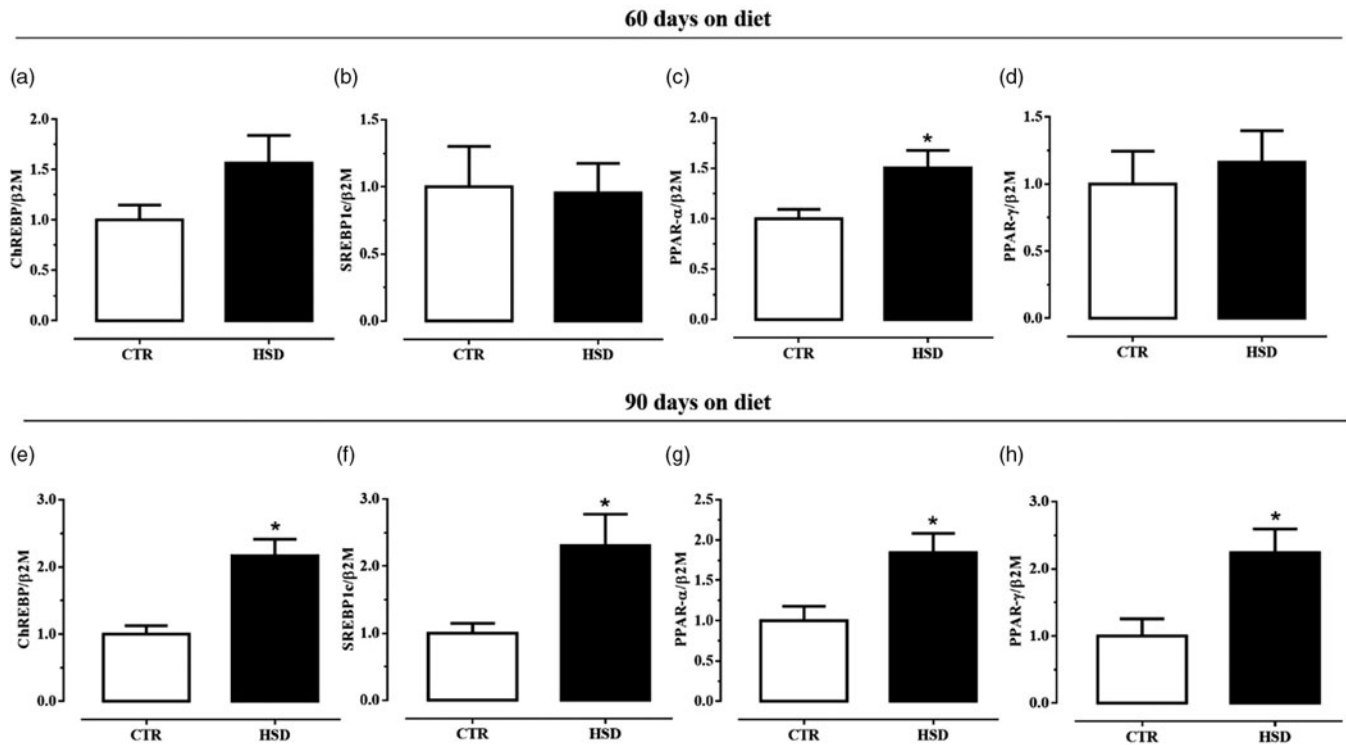


Fig. 6. Gene expression of hepatic lipogenic transcription factors. Relative mRNA expressions of carbohydrate-responsive element-binding protein (ChREBP) (a and e), sterol response element-binding protein-1c (SREBP-1c) (b and f), peroxisome proliferator-activated receptor- α (PPAR- α) (c and g) and peroxisome proliferator-activated receptor- γ (PPAR- γ) (d and h) in livers of mice fed with standard chow (CTR) and high-sucrose but isoenergetic diet (HSD) for 60 or 90 days. All samples were normalised to the relative levels of beta-2-microglobulin (β 2M), and results are expressed as the fold change values of $2^{-\Delta\Delta CT}$ as determined by qPCR. Bars represent mean \pm SEM and the difference between the groups determined by Student's *t*-test. * $p < 0.05$ vs. CTR. $n = 6$ per time per group.

hunger/satiety centres by inducing malonyl-CoA expression, which suppresses signalling pathways activated by orexigenic neuropeptides, such as neuropeptide Y and agouti-related protein.³⁰ There is additional evidence that high-sucrose but not high-fat diet induces oxytocin-mediated mechanisms which suppress certain types of feeding reward, as a kind of protection against overeating carbohydrates.³¹ Notwithstanding, increased body weight gain was likely maintained because of the effects of sucrose-derived fructose on both lipogenesis and adipogenesis. Fructose undergoes high uptake rate in both the hepatocytes³² and adipocytes,³³ where it is readily metabolised into TAG, an effect exacerbated by its co-ingestion with glucose such as in sucrose-rich diets.³⁴ In addition, fructose overload increases GLUT5 expression in WAT,³⁵ concurring for WAT hyperplasia as well as adipocyte hypertrophy.³⁶ Noteworthy, most HSD-induced metabolic disturbances are reversible by the withdrawal of excess dietary sucrose.³⁷

On the contrary, we cannot rule out the possible impact of the lower protein content in our HSD on body weight gain. Studies have shown that long-term exposure to diets containing distinct low-protein/high-carbohydrate ratios lead to increased body weight, adiposity and fatty liver, getting worse as protein goes down and carbohydrate goes high.^{38–40} Our HSD has 12.3% of its energy density as protein, which makes it a mid-protein diet instead of a low-protein diet.^{41,42} This mid-protein/high-sucrose ratio is expected to promote milder metabolic outcomes than those imposed by low-protein/HSDs, supporting the high-sucrose intake as the main contributor for higher adiposity in our HSD mice.

Ex vivo experiments showed that periepididymal WAT from HSD mice had decreased lipolysis at both basal and isoproterenol-stimulated conditions, which might concur for increased fat

mass. Dysfunctional lipolytic response to sympathetic stimulus has already been described for rodents on either sucrose²⁴ or fructose-rich⁴³ diets. Such outcome is mainly ascribed to increased catecholamine resistance on adipocyte β_2 -adrenoceptor that leads to increased stimulation of anti-lipolytic α_2 -adrenoceptors.⁴⁴ Still, impairment of insulin-dependent β -adrenergic lipolysis would play an additional role.⁴⁵ Insulin is one of the major anti-lipolytic agents acting on WAT, which acts by decreasing hormone-sensitive lipase activity in adipocytes, besides other mechanisms.³³ WAT from 90-day, but not 60-day, fed HSD mice was unresponsive to insulin stimulus, denoting an additional mechanism for their adipose tissue dysfunction. Impairment of WAT insulin sensitivity is well established for both rodents⁴⁶ and humans⁴⁷ suffering of MetS, which leads to lower FFA recycling inside the tissue and its increased secretion into bloodstream.³³ Accordingly, relative increase in serum FFA levels in 90-day-fed HSD mice, in comparison to their age-matched CTR, was twice that seen at day 60, suggesting a worse WAT dysfunction. Late development of fasting hyperglycaemia is also supported by the concurrent onset of IR on WAT. On the contrary, HSD mice did not show altered serum levels of adiponectin at any time-point. A recent prospective study with rats fed with a high-sugar diet showed that adiponectin serum levels may or may not increase depending on the time of exposure to diet.⁴⁸ Indeed, the upregulation of adiponectin expression has been associated with the onset of inflammatory response on WAT.⁴⁹ Despite the fact that we have not assessed inflammatory markers on WAT, which constitutes a limitation in our study, this set of data supports the hypothesis that insulin resistance-derived lipolysis is an early event, whereas inflammation with cytokine spillover constitutes late alterations in the course of WAT dysfunction.⁴⁹

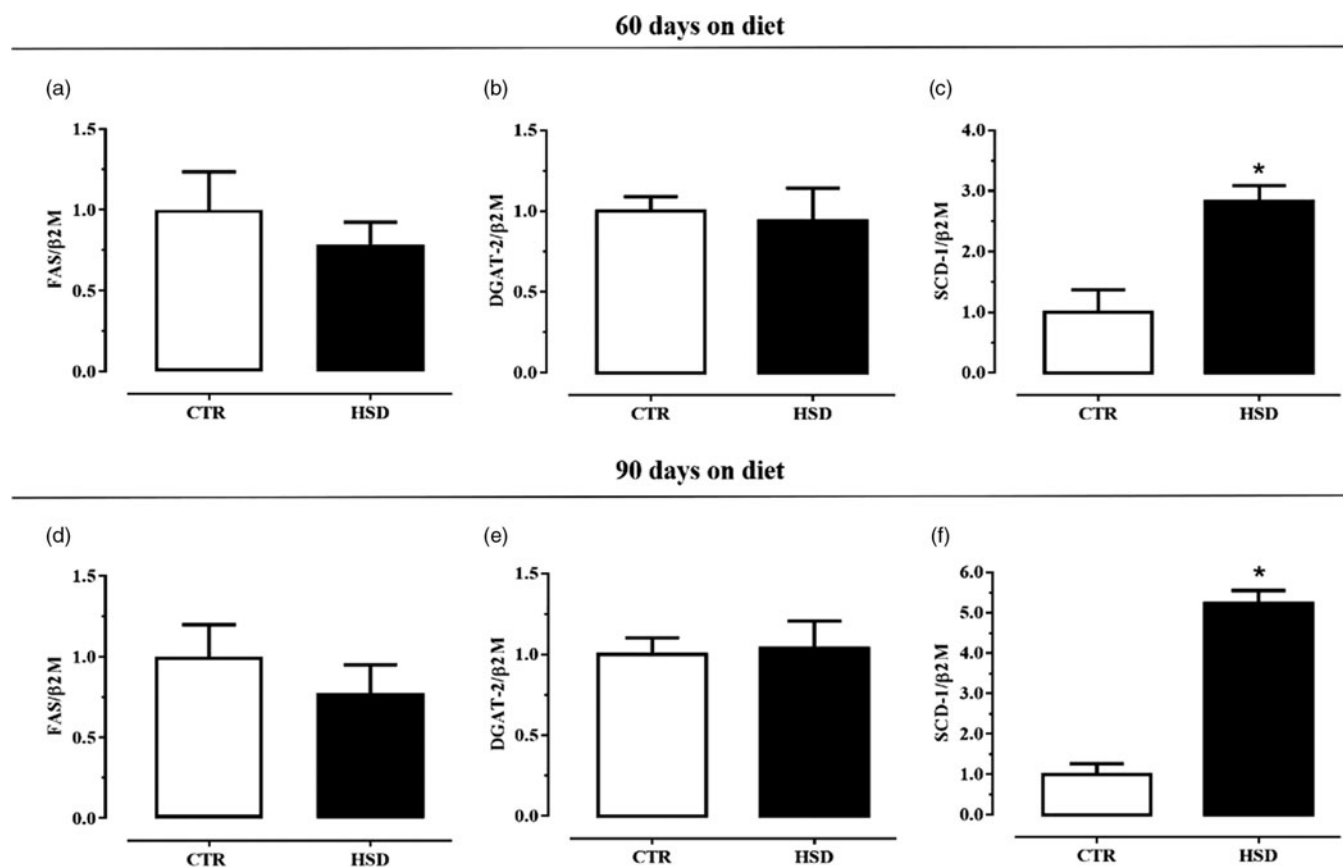


Fig. 7. Gene expression of hepatic lipogenic enzymes. Relative mRNA expressions of fatty acid synthase (FAS) (a and d), diacylglycerol acetyltransferase-2 (DGAT-2) (b and e) and stearoyl-CoA desaturase-1 (SCD-1) (c and f) in livers of mice fed with standard chow (CTR) and high-sucrose but isoenergetic diet (HSD) for 60 or 90 days. All samples were normalised to the relative levels of beta-2-microglobulin (β 2M), and results are expressed as the fold change values of $2^{-\Delta\Delta CT}$ as determined by qPCR. Bars represent mean \pm SEM and the difference between the groups determined by Student's *t*-test. * $p < 0.05$ vs. CTR. $n = 6$ per time per group.

Liver is the main recipient for FFA coming from dysfunctional WAT, where these lipids are esterified to render TAG which is stored in hepatocyte lipid droplets or incorporated into VLDL particles for secretion.⁵⁰ VLDL particles assembly and secretion is closely regulated by insulin-dependent signalling, leading to hypertriglyceridemia upon hepatic IR.⁵¹ On the contrary, fructose is rapidly metabolised by hepatocytes, leading to the upregulation of hepatic DNL and ultimate conversion of fructose itself into fatty acids.¹² Sustained DNL activation intensifies FFA-derived ectopic lipid accumulation that also impairs insulin signalling inside a vicious cycle towards NAFLD worsening.⁵² All the aforementioned set of predisposing factors was present after 60-day exposure to HSD diet because HSD mice presented increased serum and hepatic TAG levels, increased TyG Index value and simple steatosis, but no inflammatory response was verified, neither as hepatic leukocyte infiltration, nor as cytokines overexpression. TyG Index was first proposed in 2008 by Simental-Mendia et al.¹⁹ as a surrogate measure of peripheral IR in humans. Since then, it has been reliably validated in comparison to other methods, such as euglycaemic clamp and HOMA-IR,^{53–56} and consistently applied for studies in both rats^{57–60} and mice.^{13,61–63}

Next, we sought to characterise the transcriptional profile of DNL-related genes to assess the impact of both increased portal FFA levels and hepatocyte sucrose-derived fructose uptake *per se* on lipid metabolism in the liver. At day 60, HSD mice showed threefold increased *SCD-1* transcriptional levels, which coincided with increased gene expression of *PPAR- α* . *SCD-1* is

the rate-limiting enzyme catalysing TAG synthesis,⁶⁴ whereas *PPAR- α* plays a pivotal role against fatty acid-induced lipotoxicity by upregulating lipid β -oxidation pathways.⁶⁵ Such counterbalancing response probably retained steatosis worsening on HSD mice at this time-point. On the contrary, at day 90 all the assessed DNL-related transcription factors were equally upregulated on HSD mice. *SREBP-1c* and *ChREBP* are major regulators of lipid synthesis in response to hormonal and nutritional signals.¹² Both transcription factors were recently demonstrated to inter-dependently regulate lipogenic response to chronic sucrose or fructose intake.⁶⁶ In the meantime, *SCD-1* overexpression was strongly augmented to levels fivefold higher than age-matched CTR mice. We have recently described this sole upregulation of *SCD-1* gene expression in chronically HSD-fed mice.¹³ *SCD-1* has been shown to mediate the induction of *SREBP-1c* expression by chronic fructose feeding, which partially activates a positive feedback loop to further induce the expression of *SCD-1* gene and promote TAG synthesis.^{12,67} However, absence of *FASN* and *DGAT-2* induction suggests a minor role for the fructose – *SCD-1* – *SREBP-1c* axis activation, favouring the FFA-driven *SCD-1* overexpression in a *SREBP-1c*-independent pathway. This rationale is strongly supported by *in vitro* data, showing that *SCD-1* expression in HepG2 cells was increased by nearly fourfold upon incubation of 0.5 mM palmitate, an increment not changed by *SREBP-1c* silencing.⁶⁸

The consistent DNL induction verified at day 90 is seemingly responsible for the robust expansion of TAG accumulation in both serum and liver, which coincided with the progression of NAFLD

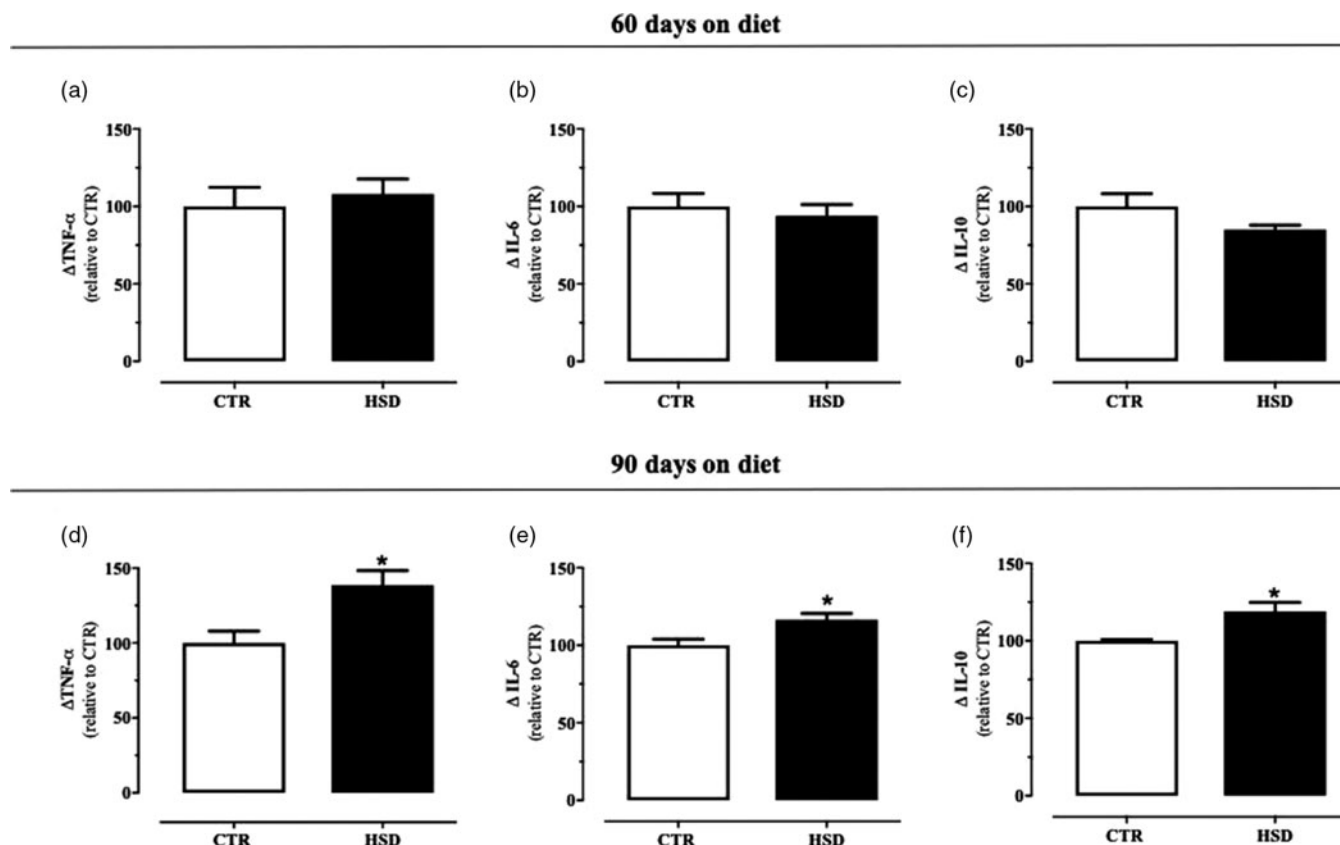


Fig. 8. Hepatic inflammatory cytokines profile. Relative levels (Δ) of tumour necrosis factor alpha (TNF- α) (a and d), interleukin 6 (IL-6) (b and e) and 10 (IL-10) (c and f) in the liver of mice fed a high-sucrose but isoenergetic diet (HSD) as compared to standard chow-fed mice (CTR) for 60 or 90 days. The bars represent mean \pm SEM and the differences between the groups were determined by Student's *t*-test. * $p < 0.05$ vs. CTR. $n = 6$ per time per group.

pattern from simple steatosis to NASH, with detectable cellular ballooning, leukocyte infiltration and local pro-inflammatory cytokines (TNF- α and IL-6) overflow. Of note, only at this time-point, HSD mice presented twofold increased hepatic transcriptional levels of *PPAR- γ* , whose ectopic overexpression in the liver has been associated with the expansion of TAG storage within lipid droplets,⁶⁹ likely to accommodate excess TAG production. Some factors are reasonably accountable for this switch. Peripheral IR *per se* is able to promote NAFLD-to-NASH progression,⁷⁰ but it does not seem to be the causal factor given 60-day-fed HSD mice had IR but no hepatic inflammation. Lipotoxicity-associated apoptosis promotes the release of damage-associated molecular patterns (DAMPs), which induce Kupffer and stellate cells to produce pro-inflammatory cytokines,^{71,72} but hepatic caspase-3 gene expression was unchanged (data not shown). On the contrary, the consistent elevation of serum FFA levels released from the dysfunctional insulin-resistant WAT is a feasible responsible for the development of NASH, apparently mediated by greater TAG storage following *SCD-1* overexpression. Sucrose and fructose have been shown to shortly and directly upregulate *SCD-1* expression,^{67,73} but the absence of hepatic inflammation in 60-day-fed HSD mice advocates for its main role on simple steatosis onset. Contrariwise, FFA has been shown both to induce *SCD-1* overexpression⁶⁸ and promote NASH development in chronically high-sucrose-fed mice in a way dependent on hepatic TNF- α expression.⁷⁴ Alike, corroborative evidence from high-fat diet-fed sirutin 1 knockout mice demonstrated that release of FFA from mesenteric adipose tissue promotes NAFLD recrudescence by induction of

hepatic lipogenesis characterised by upregulated transcriptional levels of *SREBP-1c* and *SCD-1*, but unchanged *FASN* and *DGAT-2* levels.⁷⁵

In conclusion, our study supports the onset of IR in the dysfunctional WAT with consequent increase in FFA release as a major switch factor for NAFLD-to-NASH progression in mice exposed to mid-term high-sucrose feeding from weaning through young adulthood through mechanisms presumably involving *SCD-1* overexpression in a *SREBP1-c*-independent manner. Moreover, our data are suggestive that childhood and adolescence constitute susceptible periods for fast progression of metabolic disturbances associated with added sugars consumption, as recently described for high-fat diet.⁷⁶ Last but not least, our study forewarns against early introduction of added sugars in infant diet, particularly following breast-feeding cessation.

Acknowledgements. The authors are grateful to the staff of LeFisio and LIM51 for all the technical support during experimental procedures. In particular, they are thankful to Prof. Heraldo P. de Sousa, Ph.D. and Prof. Thais M. de Lima, Ph.D. for their suggestions on some experiments.

Financial Support. This work received financial support from Fundação de Amparo à Pesquisa e ao Desenvolvimento Científico, Tecnológico e Inovação do Estado do Maranhão – FAPEMA (Universal 00643/15 and Universal 01571/16) and Coordenação de Aperfeiçoamento de Pessoal de Nível Superior – Brasil (CAPES) – Finance Code 001. PS received PIBIC fellowship from National Council for Scientific and Technological Development (CNPq). AP received Researcher fellowship from FAPEMA (BEPP-02511/18) and CNPq (308163/2019-2).

Conflicts of Interest. None.

Ethical Standards. All the procedures involving mice are in accordance with National Council for the Control of Animal Experimentation (CONCEA, Brazil) and approved by the Committee for Ethics and Welfare on Animal Use (CEUA) of the UFMA under ruling N^o 23115.002832/2017-25.

References

- Grundy SM. Metabolic syndrome update. *TRENDS CARDIOVAS MED.* 2016; 26(4), 364–373.
- Basile KJ, Johnson ME, Xia Q, Grant SF. Genetic susceptibility to type 2 diabetes and obesity: follow-up of findings from genome-wide association studies. *Int J Endocrinol.* 2014; 2014, 769671.
- Locke AE, Kahali B, Berndt SI, et al. Genetic studies of body mass index yield new insights for obesity biology. *Nature.* 2015; 518(7538), 197–206.
- Itoh H, Kanayama N. Developmental Origins of Nonalcoholic Fatty Liver Disease (NAFLD). *Adv Exp Med Biol.* 2018; 1012, 29–39.
- Lee WC, Wu KLH, Leu S, Tain YL. Translational insights on developmental origins of metabolic syndrome: focus on fructose consumption. *Biomed J.* 2018; 41(2), 96–101.
- Bray GA, Nielsen SJ, Popkin BM. Consumption of high-fructose corn syrup in beverages may play a role in the epidemic of obesity. *Am J Clin Nutr.* 2004; 79(4), 537–543.
- Bray GA. Fructose: pure, white, and deadly? Fructose, by any other name, is a health hazard. *J Diabetes Sci Technol.* 2010; 4(4), 1003–1007.
- Newens KJ, Walton J. A review of sugar consumption from nationally representative dietary surveys across the world. *J Hum Nutr Diet.* 2016; 29(2), 225–240.
- Younossi ZM, Koenig AB, Abdelatif D, Fazel Y, Henry L, Wymer M. Global epidemiology of nonalcoholic fatty liver disease—Meta-analytic assessment of prevalence, incidence, and outcomes. *Hepatology.* 2016; 64(1), 73–84.
- Chiu S, Mulligan K, Schwarz JM. Dietary carbohydrates and fatty liver disease: de novo lipogenesis. *Curr Opin Clin Nutr Metab Care.* 2018; 21(4), 277–282.
- Ipsen DH, Lykkesfeldt J, Tveden-Nyborg P. Molecular mechanisms of hepatic lipid accumulation in non-alcoholic fatty liver disease. *Cell Mol Life Sci.* 2018; 75(18), 3313–3327.
- Softic S, Gupta MK, Wang G-X, et al. Divergent effects of glucose and fructose on hepatic lipogenesis and insulin signaling. *J Clin Invest.* 2017; 127(11), 4059–4074.
- Flister KFT, Pinto BAS, Franca LM, et al. Long-term exposure to high-sucrose diet down-regulates hepatic endoplasmic reticulum-stress adaptive pathways and potentiates de novo lipogenesis in weaned male mice. *J Nutr Biochem.* 2018; 62, 155–166.
- Lafontan M. Adipose tissue and adipocyte dysregulation. *Diabetes Metab.* 2014; 40(1), 16–28.
- Fabbrini E, Sullivan S, Klein S. Obesity and nonalcoholic fatty liver disease: biochemical, metabolic, and clinical implications. *Hepatology.* 2010; 51(2), 679–689.
- de Lima DC, Silveira SA, Haibara AS, Coimbra CC. The enhanced hyperglycemic response to hemorrhage hypotension in obese rats is related to an impaired baroreflex. *Metab Brain Dis.* 2008; 23(4), 361–373.
- Bernardis L, Patterson B. Correlation between Lee index and carcass fat content in weanling and adult female rats with hypothalamic lesions. *J Endocrinol.* 1968; 40(4), 527–528.
- Suez J, Korem T, Zeevi D, et al. Artificial sweeteners induce glucose intolerance by altering the gut microbiota. *Nature.* 2014; 514(7521), 181–186.
- Simental-Mendia LE, Rodriguez-Moran M, Guerrero-Romero F. The product of fasting glucose and triglycerides as surrogate for identifying insulin resistance in apparently healthy subjects. *Metab Syndr Relat Dis.* 2008; 6(4), 299–304.
- Vaughan M. The production and release of glycerol by adipose tissue incubated in vitro. *J Biol Chem.* 1962; 237, 3354–3358.
- Freedman BD, Lee EJ, Park Y, Jameson JL. A dominant negative peroxisome proliferator-activated receptor-gamma knock-in mouse exhibits features of the metabolic syndrome. *The J Bio Chem.* 2005; 280(17), 17118–17125.
- Kleiner DE, Brunt EM, Van Natta M, et al. Design and validation of a histological scoring system for nonalcoholic fatty liver disease. *Hepatology.* 2005; 41(6), 1313–1321.
- Faul F, Erdfelder E, Lang AG, Buchner A. G*Power 3: a flexible statistical power analysis program for the social, behavioral, and biomedical sciences. *Behav Res Methods.* 2007; 39(2), 175–191.
- Pinto BAS, Melo TM, Flister KFT, et al. Early and sustained exposure to high-sucrose diet triggers hippocampal ER stress in young rats. *Metab Brain Dis.* 2016; 31, 917–927.
- D'Alessandro ME, Oliva ME, Fortino MA, Chicco A. Maternal sucrose-rich diet and fetal programming: changes in hepatic lipogenic and oxidative enzymes and glucose homeostasis in adult offspring. *Food Func.* 2014; 5(3), 446–453.
- Bouwman LMS, Fernandez-Calleja JMS, Swarts HJM, et al. No Adverse Programming by Post-Weaning Dietary Fructose of Body Weight, Adiposity, Glucose Tolerance, or Metabolic Flexibility. *Mol Nutr Food Res.* 2018; 62(2), 1700315.
- Moore JB, Gunn PJ, Fielding BA. The role of dietary sugars and de novo lipogenesis in non-alcoholic fatty liver disease. *Nutrients.* 2014; 6(12), 5679–5703.
- Kjaergaard M, Nilsson C, Rosendal A, Nielsen MO, Raun K. Maternal chocolate and sucrose soft drink intake induces hepatic steatosis in rat offspring associated with altered lipid gene expression profile. *Acta physiologica (Oxford, England).* 2014; 210(1), 142–153.
- de Queiroz KB, Coimbra RS, Ferreira AR, et al. Molecular mechanism driving retroperitoneal adipocyte hypertrophy and hyperplasia in response to a high-sugar diet. *Mol Nutr Food Res.* 2014; 58(12), 2331–2341.
- Lane MD, Cha SH. Effect of glucose and fructose on food intake via malonyl-CoA signaling in the brain. *Biochem Bioph Res Comm.* 2009; 382(1), 1–5.
- Klockars A, Levine AS, Olszewski PK. Central oxytocin and food intake: focus on macronutrient-driven reward. *Front Endocrinol (Lausanne).* 2015; 6, 65.
- Tappy L, Le KA. Metabolic effects of fructose and the worldwide increase in obesity. *Physiol Rev.* 2010; 90(1), 23–46.
- Masoodi M, Kuda O, Rossmelms M, Flachs P, Kopecky J. Lipid signaling in adipose tissue: connecting inflammation & metabolism. *Biochim Biophys Acta.* 2015; 1851(4), 503–518.
- Kolderup A, Svihus B. Fructose Metabolism and Relation to Atherosclerosis, Type 2 Diabetes, and Obesity. *J Nutr Metab.* 2015; 2015, 823081.
- Legeza B, Balazs Z, Odermatt A. Fructose promotes the differentiation of 3T3-L1 adipocytes and accelerates lipid metabolism. *FEBS Lett.* 2014; 588(3), 490–496.
- Hernandez-Diazcouder A, Romero-Nava R, Carbo R, Sanchez-Lozada LG, Sanchez-Munoz F. High Fructose Intake and Adipogenesis. *Int J Mol Sci.* 2019; 20(11), 2787.
- Sousa RML, Ribeiro NLX, Pinto BAS, et al. Long-term high-protein diet intake reverts weight gain and attenuates metabolic dysfunction on high-sucrose-fed adult rats. *Nutr Metab (Lond).* 2018; 15, 53.
- Solon-Biet SM, McMahon AC, Ballard JW, et al. The ratio of macronutrients, not caloric intake, dictates cardiometabolic health, aging, and longevity in ad libitum-fed mice. *Cell Metab.* 2014; 19(3), 418–430.
- Huang X, Hancock DP, Gosby AK, et al. Effects of dietary protein to carbohydrate balance on energy intake, fat storage, and heat production in mice. *Obesity (Silver Spring).* 2013; 21(1), 85–92.
- Sorensen A, Mayntz D, Raubenheimer D, Simpson SJ. Protein-leverage in mice: the geometry of macronutrient balancing and consequences for fat deposition. *Obesity (Silver Spring).* 2008; 16(3), 566–571.
- Jimenez-Gancedo B, Agis-Torres A, Lopez-Oliva ME, Munoz-Martinez E. Dietary protein concentration correlates in a complex way with glucose metabolism and growth performance in pregnant rats. *Domest Anim Endocrinol.* 2004; 26(4), 277–289.
- Taillandier D, Bigard X, Desplanches D, Attaix D, Guezennec CY, Arnal M. Role of protein intake on protein synthesis and fiber distribution in the unweighted soleus muscle. *J Appl Physiol (1985).* 1993; 75(3), 1226–1232.
- Rizkalla SW, Luo J, Guilhem I, et al. Comparative effects of 6 week fructose, dextrose and starch feeding on fat-cell lipolysis in normal rats: effects of

- isoproterenol, theophylline and insulin. *Mol Cell Biochem.* 1992; 109(2), 127–132.
44. Jocken JW, Blaak EE. Catecholamine-induced lipolysis in adipose tissue and skeletal muscle in obesity. *Physiol Behav.* 2008; 94(2), 219–230.
 45. Guilherme A, Henriques F, Bedard AH, Czech MP. Molecular pathways linking adipose innervation to insulin action in obesity and diabetes mellitus. *Nat Rev Endocrinol.* 2019; 15(4), 207–225.
 46. Samuel VT, Shulman GI. The pathogenesis of insulin resistance: integrating signaling pathways and substrate flux. *J Clin Invest.* 2016; 126(1), 12–22.
 47. Stanhope KL, Schwarz JM, Keim NL, *et al.* Consuming fructose-sweetened, not glucose-sweetened, beverages increases visceral adiposity and lipids and decreases insulin sensitivity in overweight/obese humans. *J Clin Invest.* 2009; 119(5), 1322.
 48. Aslam M, Madhu SV. Development of metabolic syndrome in high-sucrose diet fed rats is not associated with decrease in adiponectin levels. *Endocrine.* 2017; 58(1), 59–65.
 49. Roden M, Shulman GI. The integrative biology of type 2 diabetes. *Nature.* 2019; 576(7785), 51–60.
 50. Neuschwander-Tetri BA. Carbohydrate intake and nonalcoholic fatty liver disease. *Curr Opin Clin Nutr.* 2013; 16(4), 446–452.
 51. Kamagate A, Qu S, Perdomo G, *et al.* FoxO1 mediates insulin-dependent regulation of hepatic VLDL production in mice. *J Clin Invest.* 2008; 118(6), 2347–2364.
 52. Chen Z, Yu R, Xiong Y, Du F, Zhu S. A vicious circle between insulin resistance and inflammation in nonalcoholic fatty liver disease. *Lipids Health Dis.* 2017; 16(1), 203.
 53. Guerrero-Romero F, Simental-Mendia LE, Gonzalez-Ortiz M, *et al.* The product of triglycerides and glucose, a simple measure of insulin sensitivity. Comparison with the euglycemic-hyperinsulinemic clamp. *J Clin Endocrinol Metab.* 2010; 95(7), 3347–3351.
 54. Vasques AC, Novaes FS, de Oliveira Mda S, *et al.* TyG index performs better than HOMA in a Brazilian population: a hyperglycemic clamp validated study. *Diabetes Res Clin Pract.* 2011; 93(3), e98–e100.
 55. Irace C, Carallo C, Scavelli FB, *et al.* Markers of insulin resistance and carotid atherosclerosis. A comparison of the homeostasis model assessment and triglyceride glucose index. *Int J Clin Pract.* 2013; 67(7), 665–672.
 56. Mohd Nor NS, Lee S, Bacha F, Tfayli H, Arslanian S. Triglyceride glucose index as a surrogate measure of insulin sensitivity in obese adolescents with normoglycemia, prediabetes, and type 2 diabetes mellitus: comparison with the hyperinsulinemic-euglycemic clamp. *Pediatr Diabetes.* 2016; 17(6), 458–465.
 57. Bonfleur ML, Borck PC, Ribeiro RA, *et al.* Improvement in the expression of hepatic genes involved in fatty acid metabolism in obese rats supplemented with taurine. *Life Sci.* 2015; 135, 15–21.
 58. Rafacho A, Goncalves-Neto LM, Ferreira FB, *et al.* Glucose homeostasis in rats exposed to acute intermittent hypoxia. *Acta Physiol (Oxf).* 2013; 209(1), 77–89.
 59. Franca LM, Freitas LN, Chagas VT, *et al.* Mechanisms underlying hypertriglyceridemia in rats with monosodium L-glutamate-induced obesity: evidence of XBP-1/PDI/MTP axis activation. *Biochem Biophys Res Commun.* 2014; 443(2), 725–730.
 60. Gonzalez-Torres L, Vazquez-Velasco M, Olivero-David R, *et al.* Glucomannan and glucomannan plus spirulina added to pork significantly block dietary cholesterol effects on lipoproteinemia, arylesterase activity, and CYP7A1 expression in Zucker fa/fa rats. *J Physiol Biochem.* 2015; 71(4), 773–784.
 61. Nunes-Souza V, Cesar-Gomes CJ, Da Fonseca LJ, Guedes Gda S, Smaniotto S, Rabelo LA. Aging Increases Susceptibility to High Fat Diet-Induced Metabolic Syndrome in C57BL/6 Mice: improvement in Glycemic and Lipid Profile after Antioxidant Therapy. *Oxid Med Cell Longev.* 2016; 2016, 1987960.
 62. Shree N, Bhonde RR. Metformin preconditioned adipose derived mesenchymal stem cells is a better option for the reversal of diabetes upon transplantation. *Biomed Pharmacother.* 2016; 84, 1662–1667.
 63. Coelho CFF, Franca LM, Nascimento JR, *et al.* Early onset and progression of non-alcoholic fatty liver disease in young monosodium l-glutamate-induced obese mice. *J Dev Orig Health Dis.* 2019; 10(2), 188–195.
 64. AM AL, Syed DN, Ntambi JM. Insights into Stearoyl-CoA Desaturase-1 Regulation of Systemic Metabolism. *Trends Endocrinol Metab.* 2017; 28(12), 831–842.
 65. Gross B, Pawlak M, Lefebvre P, Staels B. PPARs in obesity-induced T2DM, dyslipidaemia and NAFLD. *Nat Rev Endocrinol.* 2017; 13(1), 36–49.
 66. Linden AG, Li S, Choi HY, *et al.* Interplay between ChREBP and SREBP-1c coordinates postprandial glycolysis and lipogenesis in livers of mice. *J Lipid Res.* 2018; 59(3), 475–487.
 67. Miyazaki M, Dobrzyn A, Man WC, *et al.* Stearoyl-CoA desaturase 1 gene expression is necessary for fructose-mediated induction of lipogenic gene expression by sterol regulatory element-binding protein-1c-dependent and -independent mechanisms. *J Biol Chem.* 2004; 279(24), 25164–25171.
 68. Bai XP, Dong F, Yang GH, Zhang L. Influences of sterol regulatory element binding protein-1c silencing on glucose production in HepG2 cells treated with free fatty acid. *Lipids Health Dis.* 2019; 18(1), 89.
 69. Yu S, Matsusue K, Kashireddy P, *et al.* Adipocyte-specific gene expression and adipogenic steatosis in the mouse liver due to peroxisome proliferator-activated receptor gamma1 (PPARgamma1) overexpression. *J Biol Chem.* 2003; 278(1), 498–505.
 70. Reccia I, Kumar J, Akladios C, *et al.* Non-alcoholic fatty liver disease: a sign of systemic disease. *Metab Clin Exp.* 2017; 72, 94–108.
 71. Farrell GC, Van Rooyen D, Gan L, Chitturi S. NASH is an inflammatory disorder: pathogenic, prognostic and therapeutic implications. *Gut Liver.* 2012; 6(2), 149.
 72. Kubes P, Mehal WZ. Sterile inflammation in the liver. *Gastroenterology.* 2012; 143(5), 1158–1172.
 73. Ntambi JM. Dietary regulation of stearoyl-CoA desaturase 1 gene expression in mouse liver. *J Biol Chem.* 1992; 267(15), 10925–10930.
 74. Feldstein AE, Werneburg NW, Canbay A, *et al.* Free fatty acids promote hepatic lipotoxicity by stimulating TNF-alpha expression via a lysosomal pathway. *Hepatology.* 2004; 40(1), 185–194.
 75. Cheng J, Liu C, Hu K, *et al.* Ablation of systemic SIRT1 activity promotes nonalcoholic fatty liver disease by affecting liver-mesenteric adipose tissue fatty acid mobilization. *Biochim Biophys Acta Mol Basis Dis.* 2017; 1863(11), 2783–2790.
 76. Cheng HS, Ton SH, Phang SCW, Tan JBL, Abdul Kadir K. Increased susceptibility of post-weaning rats on high-fat diet to metabolic syndrome. *J Adv Res.* 2017; 8(6), 743–752.